Report – Optimization and Quantization of Multibeam Beamforming Vector for Joint Communization and Radio Sensing

TECHNISCHE UNIVERSITÄT DARMSTADT

Mengshuai Zhang and Rostyslav Olshevskyi
July 1, 2022

1 Introduction

Mobile radio and radio sensing techniques have been studied for many years. But in the past, they were developed independently. In recent years, joint communication and radio sensing (JCAS, also known as integrated sensing and communication) has received much attention from researchers. Instead of having two different systems, communication and sensing functions are jointly optimized and combined in a single hardware unit. This also brings other benefits in form of reduced cost, size, weight as well as higher spectral and energy efficiencies [1].

Millimeter wave (mmWave) antennas with its high data rates can provide high resolution capability for sensing and low-latency transmission for communication systems. However, using mmWave results in an inevitable large propagation loss. Antenna arrays in combination with beamforming techniques are expected to overcome this problem by concentrating the power into the desired communication and sensing directions.

Analog array-based beamforming techniques suggested in [2] will be reproduced in this work. It will be shown that low-cost and compact analog arrays can generate the high-gain communication and sensing beams when using efficient beamforming techniques. Furthermore, we have provided our own contribution by comparing the results of two additional optimization methods.

In the first method, we start with the optimization of a single beam of a Uniform Linear Array (ULA). The pattern associated with the optimized beamforming (BF) vector is then shifted to the desired communication and sensing directions. The resulting patterns are then combined using two methods. Albeit the second method requires an additional optimization step, it is superior to the first one. Finally, we tackle the practical aspect of the problem by quantizing the optimized BF vectors making them suitable for use in analog arrays.

The rest of this report is organized as follows: we introduce the system model in Section 2, explain the multibeam optimization as well as the quantization methods in Sections 3 and 4, respectively. Eventually, we show the simulation results and draw our conclusion in the Sections 5 and 6, respectively.

2 System Model

Assume, a uniform linear array (ULA) with M elements, which are equally placed at an interval of half the carrier wavelength. The array response vector is given by

$$\mathbf{a}(\theta) = \left[1, e^{j\pi \sin(\theta)}, ..., e^{j\pi(M-1)\sin(\theta)}\right]^{\mathrm{T}}. \tag{1}$$

The channel model is considered as quasi-static for both communication and sensing. It is assumed that there are L multipath signals with AoDs $\theta_{t,l}$ and AoAs $\theta_{r,l}$, respectively. The quasi-static channel matrix between transmitter and receiver can be formulated as

$$\mathbf{H} = \sum_{l=1}^{L} b_l \delta(t-\tau_l) e^{j2\pi f_{\mathrm{D},l} t} \mathbf{a}(\theta_{t,l}) \mathbf{a}^{\mathrm{T}}(\theta_{r,l}), \tag{2}$$

where $b_l \in \mathbb{C}$ is the amplitude of l-th path, τ_l is the propagation delay, and $f_{\mathrm{D},l}$ is the associated Doppler frequency. There is only one line-of-sight (LOS) path among the L multipath, and the rest $(L-1)$ paths are non-line-of-sight (NLOS). It is also assumed that the LOS path dominates in terms of the received signal power.

The transmitted baseband signal is denoted as $s(t)$ and the transmitted and received BF vectors are $\mathbf{w}_t$ and $\mathbf{w}_r$, respectively. Then, the receive signal for sensing and communication can be represented as

$$y(t) = \mathbf{w}_r^{\mathrm{T}} \mathbf{H} \mathbf{w}_t s(t-\tau_l) + \mathbf{w}_r^{\mathrm{T}} \mathbf{z}(t) = \sum_{l=1}^{L} b_l e^{j2\pi f_{\mathrm{D},l} t} (\mathbf{w}_r^{\mathrm{T}} \mathbf{a}(\theta_{r,l}))(\mathbf{a}^{\mathrm{T}}(\theta_{t,l}) \mathbf{w}_t) s(t-\tau_l) + \mathbf{w}_r^{\mathrm{T}} \mathbf{z}(t), \tag{3}$$

where $\mathbf{z}(t)$ is the additive white Gaussian noise vector with zero mean and variance σ_n^2. Assume the mean power of the transmit signal $s(t)$ is σ_s^2. Then, the receive signal-to-noise ratio (SNR) γ can be written as

$$\gamma = \frac{||\mathbf{w}_r^{\mathrm{T}}\mathbf{H}\mathbf{w}_t||^2}{||\mathbf{w}_r||^2} \cdot \frac{\sigma_s^2}{\sigma_n^2}. \tag{4}$$

3 Multibeam Optimization

In this section, firstly we separately optimize the transmitted communication and sensing BF vectors, i.e., $\mathbf{w}_{t,c}$ and $\mathbf{w}_{t,s}$. We then combine them into the vector $\mathbf{w}_t$, which can be used for joint communication and sensing. As we will see, the obtained solution can still be improved. For this purpose, we introduce a new coefficient in order to find the optimal combination of communication and sensing beams.

3.1 Method 1

We consider the case, where the desired array response $\mathbf{v} = [v_1, ..., v_M]^{\mathrm{T}}$ for M half-wavelength-spaced, omnidirectional array elements is known such that it can be modeled as [1]

$$\mathbf{v} = \mathbf{D}_v \mathbf{p}_v, \tag{5}$$

where $\mathbf{D}_v$ is a diagonal matrix with on-diagonal elements being the desired magnitude and $\mathbf{p}_v$ is the phase of the pattern. In this case, the optimization problem can be formulated as follows

$$\mathbf{p}_{v,\mathrm{opt}} = \underset{\mathbf{p}_v}{\mathrm{argmin}}\, ||(\mathbf{A}\mathbf{A}^{\dagger} - \mathbf{I})\mathbf{D}_v\mathbf{p}_v||_2^2, \tag{6}$$

where $\mathbf{A} = [\mathbf{a}_1, ..., \mathbf{a}_K]^{\mathrm{T}}$ is the ULA response at K specified directions.

The suboptimal solution for $\mathbf{w}_{\mathrm{opt}}$ was obtained using a two-step iterative-least-squares (ILS) approach utilizing the degrees of freedom in $\mathbf{p}_v$ [3]. The optimized BF vector becomes a reference for further multibeam generation. The subbeams pointing to the desired communication and sensing directions were obtained by shifting $\mathbf{w}_{\mathrm{opt}}$ along the electrical angles. A multibeam was then computed as

$$\mathbf{w}_t = \sqrt{\rho}\mathbf{w}_{t,c} + \sqrt{1-\rho}\mathbf{w}_{t,s}, \tag{7}$$

where $\mathbf{w}_{t,c}$ and $\mathbf{w}_{t,s}$ are the BF vectors associated with communication and sensing beams, respectively, and ρ is a communication-sensing trade-off parameter. In our simulation, we used ρ=0.5. Lastly, to compare the different multibeams against each other, a set of normalized multibeams pointing to different directions were computed.

3.2 Method 2

In method 1, multibeam $\mathbf{w}_t$ is obtained by combining $\mathbf{w}_{t,c}$ and $\mathbf{w}_{t,s}$ using equation (7). However, this is not an optimal combination. For this purpose, a phase shifting term $e^{j\varphi}$ is introduced

$$\mathbf{w}_t = \sqrt{\rho}\mathbf{w}_{t,c} + \sqrt{1-\rho}e^{j\varphi}\mathbf{w}_{t,s}. \tag{8}$$

The optimization of the phase-shifting term is considered for two cases: when the channel-state information is known (subsection 3.2.1) and when only AoD is known (subsection 3.2.2).

3.2.1 Optimal Solution When $\mathbf{H}$ Is Known at Transmitter

The optimal φ, φ_{opt}, can be obtained through maximizing the receive SNR. The optimization problem is represented as

$$\varphi_{\mathrm{opt}} = \arg\max_{\varphi} \frac{||\mathbf{w}_r^{\mathrm{T}}\mathbf{H}\mathbf{w}_t||^2}{||\mathbf{w}_r||^2||\mathbf{w}_t||^2}, \tag{9}$$

with $\mathbf{w}_t = \sqrt{\rho}\mathbf{w}_{t,c} + \sqrt{1-\rho}e^{j\varphi}\mathbf{w}_{t,s}$, where $\mathbf{w}_r$ is the received BF vector. It is assumed that maximal ratio combing (MRC) is used at the receiver side. Thus, the receive BF vector becomes $\mathbf{w}_r = (\mathbf{H}\mathbf{w}_t)^*$. Then, the optimization problem can be rewritten as

$$\varphi_{\mathrm{opt}} = \arg\max_{\varphi} \frac{\mathbf{w}_t^{\mathrm{H}}\mathbf{H}^{\mathrm{H}}\mathbf{H}\mathbf{w}_t}{||\mathbf{w}_t||^2}, \tag{10}$$

with $\mathbf{w}_t = \sqrt{\rho}\mathbf{w}_{t,c} + \sqrt{1-\rho}e^{j\varphi}\mathbf{w}_{t,s}$.
By analyzing the monotonicity of the objective function, the optimal φ is given by [2]

$$\varphi_{\mathrm{opt}} = \begin{cases} \pi + \mu_0 - \gamma + 2l\pi, & \text{when } X_1 \leq 0, \\ \mu_0 - \gamma + 2l\pi, & \text{when } X_1 < 0, \end{cases} \quad \text{for } l = 0, \pm 1, \pm 2, ... \tag{11}$$

where

$$\begin{aligned}
\gamma &\triangleq \arctan(X_2/X_1),\ \mu_0 \triangleq \arcsin\left(L/\sqrt{X_1^2+X_2^2}\right),\\
X_1 &\triangleq -2P|a_1|\cos\alpha_1 + 2P|a_2|\left[\rho||\mathbf{H}\mathbf{w}_{t,c}||^2 + (1-\rho)||\mathbf{H}\mathbf{w}_{t,s}||^2\right]\cos\alpha_2,\\
X_2 &\triangleq -2P|a_1|\sin\alpha_1 + 2P|a_2|\left[\rho||\mathbf{H}\mathbf{w}_{t,c}||^2 + (1-\rho)||\mathbf{H}\mathbf{w}_{t,s}||^2\right]\sin\alpha_2,\\
L &\triangleq -4P^2|a_1||a_2|\sin(\alpha_1-\alpha_2),\\
a_1 &= |\mathbf{w}_{t,c}^{\mathrm{H}}\mathbf{H}^{\mathrm{H}}\mathbf{H}\mathbf{w}_{t,s}|, a_2 = |\mathbf{w}_{t,c}^{\mathrm{H}}\mathbf{w}_{t,s}|,\\
\alpha_1 &= \arg(\mathbf{w}_{t,c}^{\mathrm{H}}\mathbf{H}^{\mathrm{H}}\mathbf{H}\mathbf{w}_{t,s}), \alpha_2 = \arg(\mathbf{w}_{t,c}^{\mathrm{H}}\mathbf{w}_{t,s}),
\end{aligned}$$

and $P \triangleq \sqrt{\rho(1-\rho)}$.

3.2.2 Optimal Solution When Only AoD Is Known at Transmitter

In practice, it is hard to obtain full knowledge of the channel matrix. Thus, it is necessary to derive the optimal phase $\tilde{\varphi}_{\text{opt}}$ that maximizes the power at the dominating AoD θ_t. The corresponding optimization problem is given by

$$\tilde{\varphi}_{\text{opt}} = \arg\max_{\varphi} \frac{||\mathbf{a}^{\mathrm{T}}(\theta_t)\tilde{\mathbf{w}}_t||^2}{||\tilde{\mathbf{w}}_t||^2}, \tag{12}$$

with $\tilde{\mathbf{w}}_t = \sqrt{\rho}\mathbf{w}_{t,c} + \sqrt{1-\rho}e^{j\varphi}\mathbf{w}_{t,s}$. After solving the optimization problem [2], the optimal $\tilde{\varphi}$ is given by

$$\tilde{\varphi}_{\text{opt}} = \begin{cases} \pi + \tilde{\mu}_0 - \tilde{\gamma} + 2l\pi, & \text{when} \tilde{X}_1 > 0, \\ \tilde{\mu}_0 - \tilde{\gamma} + 2l\pi, & \text{when} \tilde{X}_1 < 0, \end{cases} \quad \text{for } l = 0, \pm1, \pm2, \ldots \tag{13}$$

where

$$\begin{aligned}
\tilde{\gamma} &\triangleq \arctan(\tilde{X}_2/\tilde{X}_1),\ \tilde{\mu}_0 \triangleq \arcsin\left(\tilde{L}/\sqrt{\tilde{X}_1^2+\tilde{X}_2^2}\right),\\
\tilde{X}_1 &\triangleq -2P\tilde{a}_2\tilde{a}_3\cos(\tilde{\alpha}_2+\tilde{\alpha}_3) + 2P\tilde{a}_1(\rho\tilde{a}_2^2 + (1-\rho)\tilde{a}_3^2)\cos\tilde{\alpha}_1,\\
\tilde{X}_2 &\triangleq -2P\tilde{a}_2\tilde{a}_3\sin(\tilde{\alpha}_2+\tilde{\alpha}_3) + 2P\tilde{a}_1(\rho\tilde{a}_2^2 + (1-\rho)\tilde{a}_3^2)\sin\tilde{\alpha}_1,\\
\tilde{L} &\triangleq -4P^2\tilde{a}_1\tilde{a}_2\tilde{a}_3\sin(\tilde{\alpha}_2+\tilde{\alpha}_3-\tilde{\alpha}_1),\\
\tilde{a}_1 &= |\mathbf{w}_{t,c}^{\mathrm{H}}\mathbf{w}_{t,s}|,\ \tilde{a}_2 = |\mathbf{w}_{t,c}^{\mathrm{H}}\mathbf{a}^*|,\ \tilde{a}_3 = |\mathbf{a}^{\mathrm{T}}\mathbf{w}_{t,s}|,\\
\tilde{\alpha}_1 &= \arg(\mathbf{w}_{t,c}^{\mathrm{H}}\mathbf{w}_{t,s}),\ \tilde{\alpha}_2 = \arg(\mathbf{w}_{t,c}^{\mathrm{H}}\mathbf{a}^*),\ \tilde{\alpha}_3 = \arg(\mathbf{a}^{\mathrm{T}}\mathbf{w}_{t,s}).
\end{aligned}$$

4 Quantization of Multibeam Beamforming Vector

Most of the optimized BF vector $\mathbf{w}_t$ cannot be realized in a practical analog array. Indeed, it must be transformed into predefined discrete phase values. In this section, we will quantize the BF vector $\mathbf{w}_t$ using single (1-PS) and double (2-PS) phase shifters, respectively.

4.1 One Phase Shifter

Each element of $\mathbf{w}_t$ is of the form $w_i = |w_i|e^{j\psi_i}$, $i = 1, ..., M$, where ψ_i is the phase of w_i. In the 1-PS array, the phase of each element of the BF vector $\mathbf{w}_t$ can be calculated by

$$\hat{\beta}^{(i)} = \arg\min_{\hat{\beta}\in\mathcal{B}} |\mathrm{mod}_{2\pi}(\psi_i - \hat{\beta})|, \tag{14}$$

where $\hat{\beta} \in \mathcal{B} = \{0, \triangle_\beta, 2\triangle_\beta, ..., (2^b-1)\triangle_\beta\}$ with quantization step $\triangle_\beta = 2\pi/2^b$, and b is the number of quantization bits.

A 1-PS matches each element of the BF vector with a predefined phase value, but all elements will have the same amplitude. While it is a simple way to quantize the BF vector, it results in undesirable sidelobes due to amplitude mismatching.

4.2 Two Phase Shifters

To solve the issue mentioned above, we can utilize a 2-PS scheme. Two phase shifters are able to represent the elements of BF vectors with much smaller error than 1-PS. For two phase shifters, there are three methods for calculating the phase shifting values.

4.2.1 Separate Quantization of Individual Phase Shifters

According to [2], the elements w_i of BF vector $\mathbf{w}$ can be rewritten as

$$w_i = |w_i| e^{j\psi_i} = e^{j\beta_1^{(i)}} + e^{j\beta_2^{(i)}}, \tag{15}$$

so that $\beta_1^{(i)}$ and $\beta_2^{(i)}$ can be quantized separately into

$$\begin{aligned} \hat{\beta}_1^{(i)} &= \arg\min_{\hat{\beta}_1 \in \mathcal{B}_1} |\text{mod}_{2\pi}(\beta_1^{(i)} - \hat{\beta}_1)|, \\ \hat{\beta}_2^{(i)} &= \arg\min_{\hat{\beta}_2 \in \mathcal{B}_2} |\text{mod}_{2\pi}(\beta_2^{(i)} - \hat{\beta}_2)|, \end{aligned} \tag{16}$$

where $\hat{\beta}_1 \in \mathcal{B}_1 = \left\{0, \triangle_{\beta_1}, 2\triangle_{\beta_1}, ..., (2^{b_1} - 1)\triangle_{\beta_1}\right\}$ and $\hat{\beta}_2 \in \mathcal{B}_2 = \left\{0, \triangle_{\beta_2}, 2\triangle_{\beta_2}, ..., (2^{b_2} - 1)\triangle_{\beta_2}\right\}$ are the sets of the quantized phase values.

4.2.2 Joint Quantization Using Combined Quantization Codebooks

In joint quantization scheme, the codebook $\mathcal{C}$ with code $\hat{c_j}$ is generated by combining two sets of the quantized phase values with equation $\hat{c_j} = e^{j\hat{\beta}_1} + e^{j\hat{\beta}_2}$, where $\hat{c_j}$ is the j-th element of $\mathcal{C}$. Two separate codebooks are defined as

$$\begin{aligned} \hat{\beta}_1 \in \mathcal{B}_1 &= \left\{0, \triangle_{\beta_1}, 2\triangle_{\beta_1}, ..., (2^{b_1} - 1)\triangle_{\beta_1}\right\}, \\ \hat{\beta}_2 \in \mathcal{B}_2 &= \left\{\phi, \phi + \triangle_{\beta_2}, ..., \phi + (2^{b_2} - 1)\triangle_{\beta_2}\right\}, \end{aligned} \tag{17}$$

where $\phi \in [0, \triangle_{\beta_2}/2]$ is a constant.

The constellation points $\hat{c_j}$ are normalized so that $\text{E}[|\hat{c_j}|^2] = 1/M$. Then each BF weight w_i can be obtained by

$$\hat{w}_i = \arg\min_{\hat{c_j} \in \mathcal{C}} |w_i - \hat{c_j}|^2. \tag{18}$$

4.2.3 Quantization With Optimized Scaling Factor

In a joint quantization scheme, the normalization factor depends on the number of bits b and the dimension of the array M. In order to normalize the BF vector with an optimal factor, we can use the, so-called IGSS-Q algorithm, which is based on the improved golden section search (IGSS) algorithm [4].

The IGSS-Q method aims to find the optimal normalization factor υ_{opt} by iteratively solving

$$\upsilon_{\text{opt}} = \arg\min_{\upsilon} ||\upsilon \mathbf{w}_t - \hat{\mathbf{q}}(\upsilon)||_2^2, \tag{19}$$

in which $\hat{q}(\upsilon)$ is updated in each iteration through

$$\hat{q}_i = \arg\min_{\hat{c_j} \in \mathcal{C}} |\upsilon w_i - \hat{c_j}|^2. \tag{20}$$

In the beginning of IGSS-Q, a searching interval $[a_1, a_2]$ is initialized. According to the inital value of a_1 and a_2, two interior points x_1 and x_2 within the search interval are determined . In each iteration, the errors of these four point are computed through

$$e(x) = \sum_{i=1}^{M} |x w_i - \hat{q}_i|^2. \tag{21}$$

By finding the smallest error among $e(a_1)$, $e(a_2)$, $e(x_1)$ and $e(x_2)$, the length of search interval decreases iteratively. When $|e(a_1) - e(a_2)|$ is smaller than a threshold, or the iteration time exceeds a given constant, then the algorithm stops, and the optimal factor υ_{opt} is determined as either a_1 or a_2.

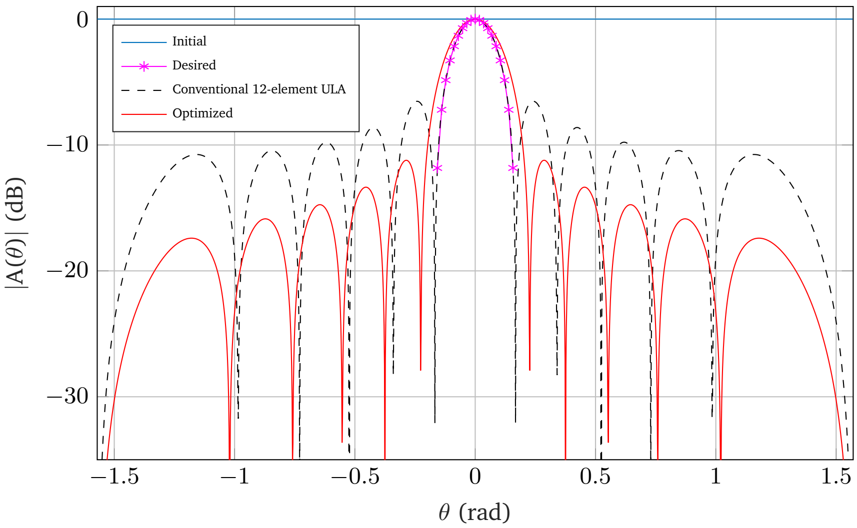

Figure 1: Normalized magnitude pattern used in the optimization process.

5 Simulation

A set of beams used in two-step ILS algorithm is depicted in the Figure 1. The initial BF matrix has been set to $\mathbf{D}_v = \mathbf{I}$. The desired magnitude pattern was computed from the conventional 12-element ULA response by setting all sidelobes to 0. Note that the optimized beam obtains a lower side-lobe-level in comparison to the conventional one, which is a desired effect. A multibeam BF vector was computed as a weighted sum of the communication and sensing BF vectors. The normalized multibeam with the communication subbeam pointing to the boresight direction can be seen in the Figure 2. Since the sensing beam was optimized with respect to an electrical angle unequal to 0, mapping the corresponding BF vector to the elevation cut broadens the subbeam. The advantage of this side-effect is a larger sensing area. The resolution capability will deteriorate, though.

After that, a set of normalized multibeams with the sensing beams pointing to directions different from 0 was generated and is shown in Figure 3. During optimization, we have followed a general practice and spaced the scanning subbeams by 3 dB. The spacing was computed from $\sin^{-1}(\frac{1.2}{M})$. Practically speaking, the corresponding BF vectors can be computed offline, saving computational resources and reducing the latency during the packet transmission.

Figure 4 shows how the normalized powers at the receiver and at the dominating AoD change with φ varying between -180° and 180°. The power is normalized to the value obtained when a single communication beam pointing to the dominating AoD is used. The communication beam and sensing beam are fixed at 0° and 10.8°, respectively. It can be seen that, the power associated with the optimal φ computed as in (10) and (12), are exactly at the peak of their corresponding normalized powers. Moreover, the variance of power at Rx for 'H-known' is larger than the power at the dominating AoD for 'AoD-known'. It is also notable that there is a bias between the optimized φ obtained in the 'H-known' case and 'AoD-known' case, respectively. Therefore, the maximum received power cannot be reached in 'AoD-known'. That is why in Figure 5 the received power corresponding to the optimized φ in 'H-known' (red solid line) is always bigger than than φ in 'AoD-known' (blue solid line) with increasing ρ. The received power associated with φ in method 1, i.e., $\varphi = 0$, is smallest over ρ.

In Figure 6, we compare the beamforming radiation patterns with quantization from 1-PS and joint quantization from 2-PS. The communication beam is pointing at 0°, and the sensing beam is fixed at -12.3°. Both subbeams are generated in analog antenna arrays having 16 elements. In 1-PS quantization, fast block noncoherent decoding (FBND)[5] is used to solve problem (14). The codebooks $\mathcal{C}_1$ and $\mathcal{C}_2$ for joint quantization are using $\phi = 0$ and $\phi = \triangle_{\beta_2}/2$, respectively. In 1-PS quantization, the sidelobe of the quantized BF vector does not match the non-quantized one, even when the number of quantization bits has increased to $b = 4$. This is caused by the mismatch of the amplitudes when using 1-PS. However, the joint quantization for 2-PS receives better performance than 1-PS. Indeed, we obtain similar BF radiation patterns as non-quantized BF vector with $\mathcal{C}_1$ or $\mathcal{C}_2$, when the number of bits reaches 4.

6 Conclusions

In this project we have reproduced the results for multibeam optimization using two methods. In method 1, the sub-optimal communication and sensing beams are obtained separately by minimizing the difference between the desired and the optimized beam patterns. The weighted communication and sensing BF vectors were then summed up resulting into a BF vector $\mathbf{w}_t$. Method 2 focuses on finding a optimal combination of multibeam to gain maximum received power in the case when channel state information

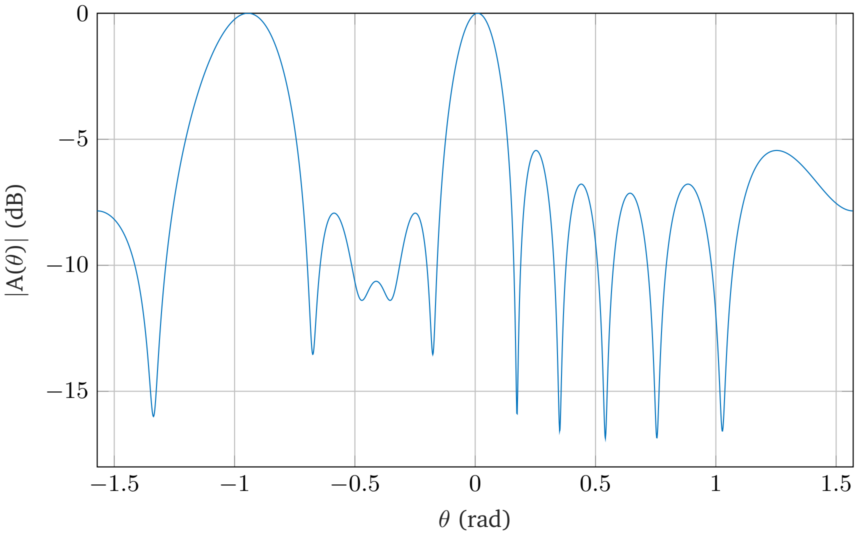

Figure 2: An optimized multibeam.

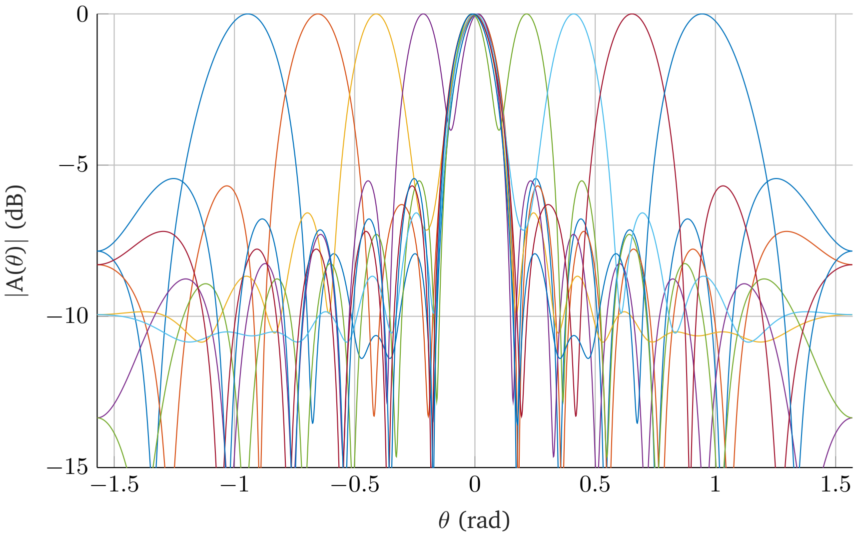

Figure 3: A set of normalized optimized multibeams, $M = 12$, $\delta = 0.2$.

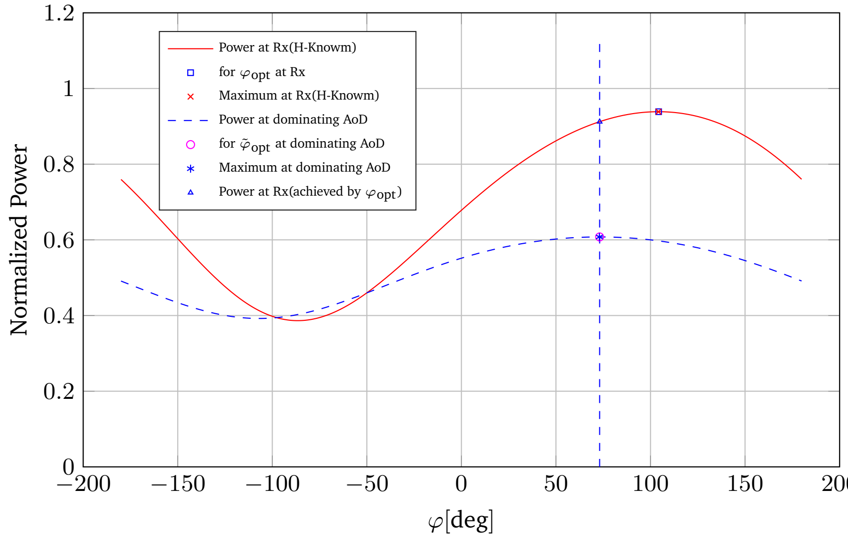

Figure 4: Normalized signal power at the receiver (Rx) and at the dominating AoD versus combining phase φ.

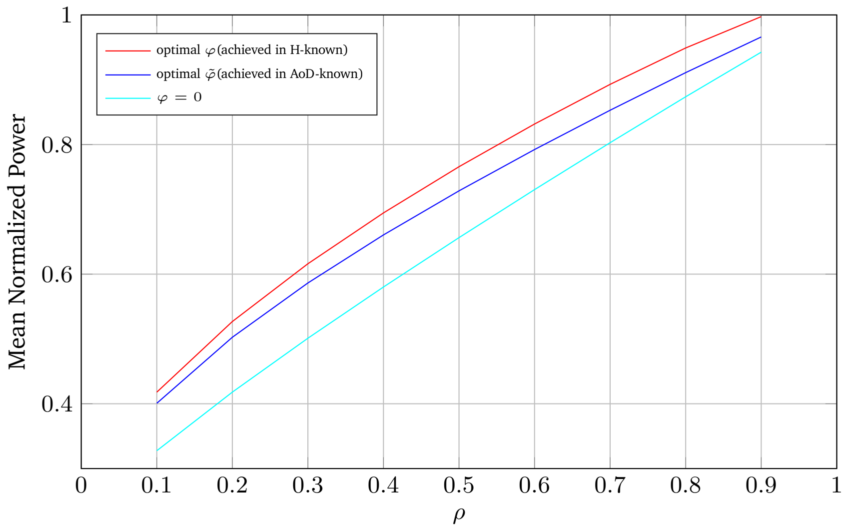

Figure 5: Normalized mean received signal power at the receiver (Rx) versus power distribution factor ρ for optimized and non-optimal φ.

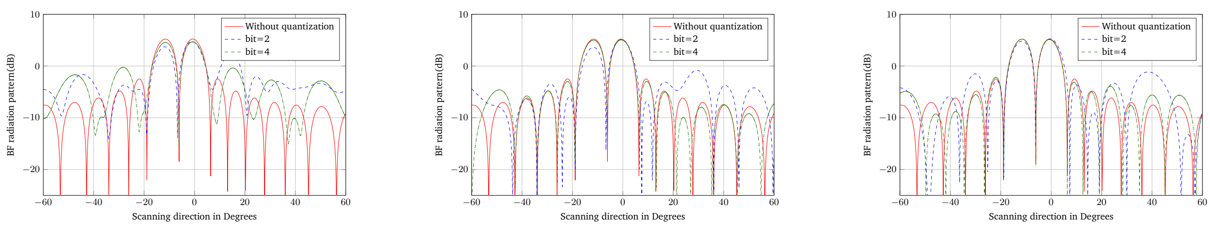

(a) FBND quantization for 1-PS. (b) Joint quantization for 2-PS with Codebook $\mathcal{C}_1$. (c) Joint quantization for 2-PS with Codebook $\mathcal{C}_2$.

Figure 6: BF radiation pattern for different number of quantization bits.

or AoD is known. The obtained beams were quantized with 1-PS and 2-PS. Three different methods for 2-PS were investigated. According to the simulation results, BF vectors quantized with 2-PS outperform the one with 1-PS.

An interesting research direction is to verify how the optimization algorithms perform with the array different from ULA. Furthermore, the optimized beam obtained by the two-step ILS is sub-optimal, since during the optimization, the phase value had to be manually mapped on the unit circle. It is of interest to study whether the optimal solution for this problem can be obtained. Finally, we only used the codebook $\mathcal{C}_1$ and $\mathcal{C}_2$ with shift $\phi = 0$ and $\phi = \triangle_{\beta_2}/2$, respectively, for joint quantization. However, the shift ϕ could take any values from 0 to $\phi = \triangle_{\beta_2}/2$. Therefore, it is also of interest to verify whether there exists a ϕ which can be used in creating an optimal codebook for quantization.

References

[1] J. Andrew Zhang et al. "Multibeam for Joint Communication and Sensing Using Steerable Analog Antenna Arrays". In: (2018), p. 5.

[2] Z. Shi and Z. Feng. "Optimization and Quantization of Multibeam Beamforming Vector for Joint Communication and Radio Sensing". In: IEEE TRANSACTIONS ON COMMUNICATIONS 67.9 (2019).

[3] Z. Shi and Z. Feng. "A new array pattern synthesis algorithm using the two-step least-squares method". In: IEEE Signal Processing Letters 12.3 (2005), pp. 250–253.

[4] E. Höpfinger. "On the solution of the unidimensional local minization problem". In: Journal of Optimization Theory and Applications 18.3 (1976), pp. 425–428. DOI: 10.1007/BF00933821.

[5] W. Sweldens. "Fast block noncoherent decoding". In: IEEE Communications Letters 5.4 (2001), pp. 132–134. DOI: 10.1109/4234.917091.